IEICE TRANS. COMMUN., VOL. E83-B, NO. 9 SEPTEMBER 2000

PAPER Special Issue on Advances in Radar Systems

Three-Dimensional Fully Polarimetric Imaging in Snowpack by a Synthetic Aperture FM-CW Radar

Toshifumi MORIYAMA†*, Yoshio YAMAGUCHI†, *and* Hiroyoshi YAMADA†, *Regular Members*

SUMMARY This paper presents a three-dimensional polarimetric detection result of targets buried in snowpack by synthetic aperture FM-CW radar system. Since the FM-CW radar is suitable for short range sensing and can be equipped with fully polarimetric capability, we further extended it to a polarimetric three-dimensional SAR system. A field experiment was carried out to image and detect targets in a natural snowpack of 280 cm deep. The polarimetric detection and identification schemes are the polarimetric filtering, three-component decomposition, and the power polarization anisotropy coefficient. These approaches to acquired data show the usefulness of three-dimensional polarimetric FM-CW SAR system.

***key words**: radar polarimetry, FM-CW radar, power polarization anisotropy coefficient, three-component decomposition technique, polarimetric filtering*

1. Introduction

This paper discusses the three-dimensional polarimetric imaging in a natural snowpack by synthetic aperture FM-CW radar. Since the FM-CW radar is suitable for short range sensing, it is convenient to detect targets buried in the ground and/or in the snowpack. The FM-CW radar can be extended to a synthetic aperture radar system [1], to a fully polarimetric radar [2], and to a real-time system [3]. It has been confirmed in a laboratory that the FM-CW radar can be equipped with fully polarimetric capability, and provides precise scattering matrix elements, and is useful for polarimetric imaging [2]. We further extended it to a three-dimensional polarimetric FM-CW SAR system to detect targets buried in snowpack. It is our purpose to show the usefulness of three-dimensional polarimetric FM-CW SAR.

This paper briefly describes the principles of the three-dimensional synthetic aperture processing in Sect. 2, principles of radar polarimetry in Sect. 3, including polarimetric filtering, power polarization anisotropy coefficient classifier, together with three component decomposition. These polarimetric approaches are collaboratory devoted to retrieve information obtained by the experimental data. Section 4 demonstrates the snowpack field measurements for three-dimensional imaging of embedded targets, polarimetric classification and identification results, obtained by the radar system. It is confirmed that the developed system is effective for short range sensing, especially for polarimetric detection of objects in snowpack, etc.

Manuscript received January 7, 2000.
Manuscript revised March 27, 2000.

† The authors are with Niigata University, Niigata-shi, 950-2181 Japan.
* Presently, with Fujitsu System Integration Laboratories Ltd.

2. Principle of Three-Dimensional Synthetic Aperture FM-CW Radar

An FM-CW radar measures a distance between the antenna and target by beat signal of transmitted and received signal. The transmitted signal is linearly swept from $f_0 - \frac{\Delta f}{2}$ to $f_0 + \frac{\Delta f}{2}$ where f_0 is the center frequency and Δf is the bandwidth of the transmitted signal. If a target, whose point target reflection coefficient function is given by $g\,(x_0, y_0, z_0)$, is located at distance r_b from the transmitted antenna in the three-dimensional space, the beat spectrum S_b can be written as

$$S_b = g\,(x_0, y_0, z_0)\; p\,(x - x_0, y - y_0, z_0)\; \mathrm{sinc}[\alpha(z - r_b)] \tag{1}$$

$$\alpha = \frac{2\pi\Delta f\sqrt{\varepsilon_r}}{c}$$

$$p\,(x - x_0, y - y_0, z_0) = \exp\left[j\frac{4\pi f_0\sqrt{\varepsilon_r}}{c}r_b\right]$$

$$r_b = \sqrt{(x - x_0)^2 + (y - y_0)^2 + z_0^2}$$

where c and ε_r are the velocity of light and relative permittivity, p is propagation function, and sinc is $\frac{\sin(x)}{x}$. If transmitting and receiving antennas are scanned on a two-dimensional x-y plane, the following procedure makes three-dimensional image. The beat spectrum received at the antenna position $(x,y,0)$ by two-dimensional antenna scan can be written as

$$S_b(x, y, z) = \int_0^{\infty}\int_{-\infty}^{\infty}\int_{-\infty}^{\infty} g(x_0, y_0, z_0)\, p(x - x_0, y - y_0, z_0) \cdot \mathrm{sinc}[\alpha(z - r_b)]\, dx_0\, dy_0\, dz_0\,. \tag{2}$$

At $z = z_0$, the beat spectrum can be rewritten as

$$S_b(x, y, z_0) = \int_{-\infty}^{\infty}\int_{-\infty}^{\infty} g\,(x_0, y_0, z_0) \cdot p\,(x - x_0, y - y_0, z_0)\, dx_0\, dy_0\,. \tag{3}$$

The reflection coefficient distribution function can be obtained by an inverse Fresnel transform

$$g(x_0, y_0, z_0) = \int_{-L_y/2}^{L_y/2} \int_{-L_x/2}^{L_x/2} S_b(x, y, z_0) \cdot p^*(x_0 - x, y_0 - y, z_0)\, dx\, dy \quad (4)$$

where L is the antenna scan width. The symbol * denotes complex conjugation. Therefore, execution of Eq. (4) with respect to range z-direction yields a three-dimensional image.

3. Brief Principle of Radar Polarimetry

In the polarimetric FM-CW radar [2], if the polarimetric measurement is conducted in the HV polarization basis, the set of polarimetric monostatic complex reflection coefficient (g_{HH}, g_{HV} and g_{VV}), given in Eq.(4), provides a scattering matrix $[S(HV)]$.

$$[S(HV)] = \begin{bmatrix} S_{HH} & S_{HV} \\ S_{HV} & S_{VV} \end{bmatrix} = \begin{bmatrix} g_{HH} & g_{HV} \\ g_{HV} & g_{VV} \end{bmatrix} \quad (5)$$

If the scattering matrix $[S(HV)]$ is given, it is possible to synthesize the received power P at any polarization state.

$$\mathbf{E}_s(HV) = [S(HV)]\, \mathbf{E}_t(HV) \quad (6)$$

$$P = \left| \mathbf{h}(HV)^{\mathrm{T}} \mathbf{E}_s(HV) \right|^2 = \left| \mathbf{h}(HV)^{\mathrm{T}} [S(HV)]\, \mathbf{E}_t(HV) \right|^2 \quad (7)$$

where $\mathbf{E}_t$ and $\mathbf{E}_s$ is transmitted wave from antenna and scattering wave from target, respectively. The superscript T denotes transpose and $\mathbf{h}$ is the polarization state of the radar receiver expressed in terms of the polarization ratio ρ defined by

$$\mathbf{h} = \frac{1}{\sqrt{1 + \rho\rho^*}} \begin{bmatrix} 1 \\ \rho \end{bmatrix}. \quad (8)$$

Since polarimetric synthetic aperture image consists of the scattering matrix, it is possible to re-calculate the image at any polarization state by Eq. (7).

There are many radar polarimetry applications such as target enhancement, classification, and interferometry, etc. We employed polarimetric filtering [4], [5], power polarization anisotropy coefficient [6] and the three-component decomposition technique [7] for the effective detection and identification of targets in snowpack.

3.1 Polarimetric Filtering

We define a contrast enhancement factor by the power ratio as

$$C = \frac{P\,(\text{Power of target 1})}{P\,(\text{Power of target 2})} = \frac{\left| \mathbf{h}(HV)^{\mathrm{T}} [S_1(HV)]\, \mathbf{E}_t(HV) \right|^2}{\left| \mathbf{h}(HV)^{\mathrm{T}} [S_2(HV)]\, \mathbf{E}_t(HV) \right|^2}. \quad (9)$$

The subscript 1 corresponds to a desired target for which we wish to enhance and the subscript 2 corresponds to undesired target to be eliminated. The optimal polarization state which maximizes the contrast factor of desired target is the null polarization of undesired target. In Co-pol channel case ($\mathbf{h} = \mathbf{E}_t$), this is analytically derived from

$$C = \infty \; : \; P\,(\text{Power of target 2}) = \left| \mathbf{E}_t(HV)^{\mathrm{T}} [S_2(HV)]\, \mathbf{E}_t(HV) \right|^2 = 0. \quad (10)$$

The null polarization states are given by [4]

$$\rho_{cn,2} = \frac{-S_{2,HV} \pm \sqrt{S_{2,HV}^2 - S_{2,HH} S_{2,VV}}}{S_{2,VV}}. \quad (11)$$

The null-polarization state imaging will eliminate undesired target, provided certain area occupied by the radar target had similar scattering matrices.

3.2 Power Polarization Anisotropy Coefficient

The scattering matrix has two invariants regardless of the polarization basis which can be related to its eigenvalues λ_1 and λ_2. The first invariant is the span, i.e., the sum of the square of scattering matrix elements

$$Span[S(HV)] = |S_{HH}|^2 + 2|S_{HV}|^2 + |S_{VV}|^2 = |\lambda_1|^2 + |\lambda_2|^2. \quad (12)$$

The second invariant is the determinant of scattering matrix

$$\left| Det[S(HV)] \right| = \left| S_{HH} S_{VV} - S_{HV}^2 \right| = |\lambda_1 \lambda_2|. \quad (13)$$

The power polarization anisotropy coefficient μ is defined in terms of these two invariants as follows,

$$\mu = \sqrt{1 - 4 \left| \frac{Det[S]}{Span[S]} \right|^2} = \frac{|\lambda_1|^2 - |\lambda_2|^2}{|\lambda_1|^2 + |\lambda_2|^2}, \quad |\lambda_1| \geq |\lambda_2|, \; 0 \leq \mu \leq 1. \quad (14)$$

If the power polarization anisotropy coefficient μ is equal to 0, the target is isotropic target (such as sphere or plate). On the other hand, if this coefficient is close to 1, the target is anisotropic target (such as a straight wire or a helical target) or any other polarimetrically sensitive target.

These invariants contribute to classification of man-made targets, especially in a case such that the precise polarization state is difficult to define because of near range or in an inhomogeneous medium.

Table 1 Contribution of magnitude factors for fundamental targets.

	K_s	K_d	K_h
sphere, plate	1	0	0
diplane	0	1	0
line(wire)	0.5	0.5	0
right / left > helix	0	0	1

3.3 Three-Component Decomposition Technique

In the monostatic radar case, the off-diagonal elements of the scattering matrix are identical with each other. It is possible to decompose the scattering matrix into three components, as if the target consists of a sphere, a diplane and a right or left helix.

$$[S(HV)] = \begin{bmatrix} S_{HH} & S_{HV} \\ S_{HV} & S_{VV} \end{bmatrix}$$

$$= e^{j\varphi}\left\{ K_s \begin{bmatrix} 1 & 0 \\ 0 & 1 \end{bmatrix} + e^{j\varphi_r} \left\{ \begin{array}{l} K_d \begin{bmatrix} \cos 2\theta & \sin 2\theta \\ \sin 2\theta & -\cos 2\theta \end{bmatrix} \\ + K_h \begin{bmatrix} 1 & \pm j \\ \pm j & 1 \end{bmatrix} \end{array} \right\} \right\}. \quad (15)$$

where K_s, K_d and K_h show the magnitude of the fundamental scattering matrix corresponding to a sphere (odd bounce reflection target), a diplane (even bounce reflection target) and a helix, respectively. Each contribution is given by

$$\frac{K_i}{K_s + K_d + K_h}, \ (i = s, d, h). \quad (16)$$

The three-component decomposition can be utilized to classify a target into four basic types based on Eq.(16) and as shown in Table 1. The decomposition technique can be carried out easily in the circular *LR* basis[4].

Since this decomposition directly applies to the scattering matrix data, it is very fast approach to classify and identify radar targets and is suitable for a real-time classifier.

4. Three-Dimensional Polarimetric Imaging in Snowpack

In order to confirm the usefulness of three-dimensional polarimetric imaging, we carried out an experiment to detect targets in natural snowpack at Yamakoshi village, Niigata prefecture, Japan on Feb. 2, 1997. The measurement specifications are shown in Table 2. Since the L-band wave can penetrate deeply into snowpack, we used a rectangular horn antenna operating from 1.1 to 2.2 GHz. The snow structure is illustrated in Fig. 1. The snowpack consisted of some snow layers (new snow, fine grained snow and depth hoar layer). The average relative permittivity of snowpack was 1.5. The targets were used a metallic cylinder of 3 cm diameter and

Table 2 Measurement specifications.

Radar system	FM-CW
Transmitted center frequency	1.65 GHz
Transmitted frequency width	1.1 GHz
Sweep time	5.1 msec
Antenna type	Rectangular horn
Measurement point	64 × 64
Measurement interval	2 cm
Average relative permittivity of snow	1.5
Measurement polarization	HH,HV,VV

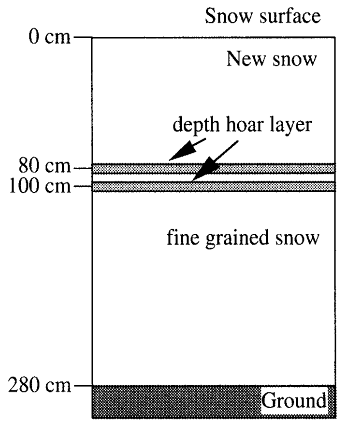

Fig. 1 Structure of snowpack.

180 cm long (target 1), and a metallic plate bar of 4 cm wide and 180 cm long (target 2), respectively. The transmitting and receiving antennas were scanned two-dimensionally on the snow surface to acquire the three-dimensional image. The number of sampling points both in the *x*- and *y*-directions is 64×64, with incremental width of 2.0 cm. Moreover, polarimetric measurement was conducted to obtain the scattering matrix element (*HH*, *HV* and *VV* where *H* stands for polarization direction being parallel to the *x*-direction, and *V* to the *y*-direction, respectively).

4.1 Experiment 1

The measurement situation is depicted in Fig. 2. The target 1 was buried at a depth of 60 cm and oriented 45 degree with respect to the *y*-direction. The target 2 was buried at a depth of 110 cm and orthogonal to target 1. Since three-dimensional volume data acquisition was conducted, it is possible to slice the data at any depth. The *VV* polarization detection result of target 2 is shown in Fig. 3. This result is a real aperture slice image at the depth of 110 cm. Although the image is unfocused in Fig. 3, the synthetic aperture processing yields focused image in Fig. 4. The target appears more clearly than the real aperture image. The two-dimensional (*x*-*y*) SAR processing with respect to a range (*z*) direction yields three-dimensional SAR images as shown in Fig. 5. These images was obtained with the same threshold level. It is easy to recognize the situation of buried targets and see the inhomogeneity within the snowpack under the depth of 170 cm. Moreover, we can see the position of ground surface in these images. Since the synthetic aperture processing can not focus the ground surface correctly due to the inhomogeneity of snowpack, this surface is not smooth. However, this three-dimensional FM-CW SAR is useful to examine inhomogeneous medium such as snowpack and ground.

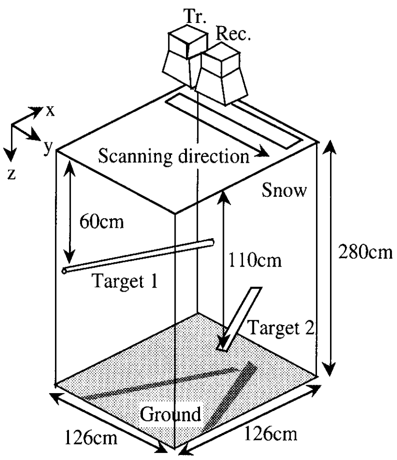

Fig. 2 Measurement situation 1.

In order to verify the effectiveness of polarimetric filtering principle to three-dimensional data, we tried to produce an image which enhances the target 2 against target 1. Figure 6 shows the Co-pol null image of target 1 by Eq.(11). Since polarimetric filtering suppress the target 1, the maximum contrast image for target 2 is obtained. The polarimetric filtering is available and useful to the three-dimensional polarimetric experimental data.

4.2 Experiment 2

The measurement situation 2 is depicted in Fig. 7. In this experiment, two targets (target 1 and 2) were buried at a depth of about 100 cm. Figure 8 is the three-dimensional SAR images. The cylinder target (target 1) is detected in the *HH*, *HV* and *VV* images. However, the center part of the image disappeared due to inhomogeneity of snowpack.

In this situation, we attempted to extract the polarimetric information of each target. Figure 9 shows the three-component decomposition result for classification and identification of target. The cylinder target in the air has theoreti-

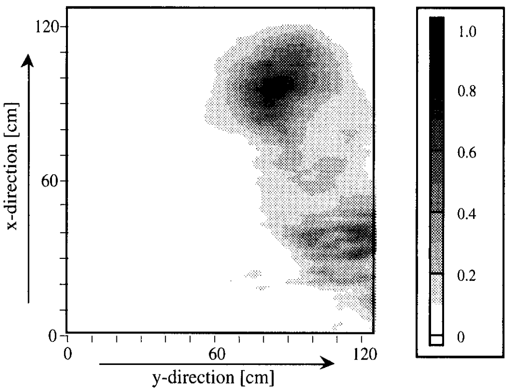

Fig. 3 Real aperture image of target 2 at the depth of 110 cm (VV).

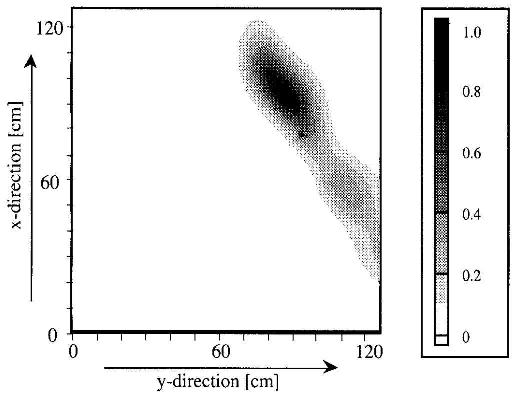

Fig. 4 Synthetic aperture image of target 2 at the depth of 110 cm (VV).

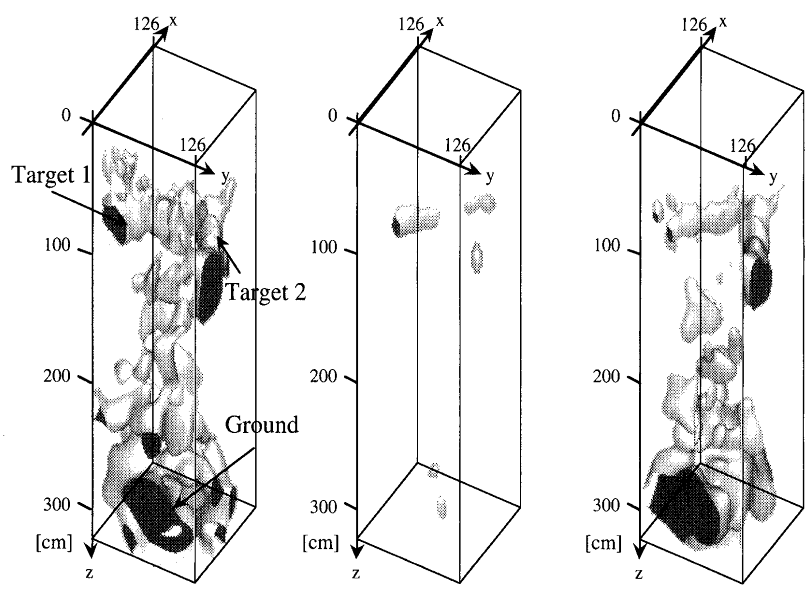

(a) HH (b) HV (c) VV

Fig. 5 Three-dimensional image of experiment 1.

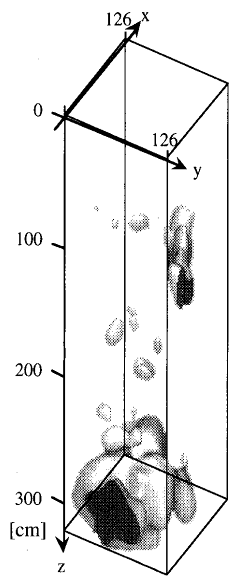

Fig. 6 Co-pol null of target 1.

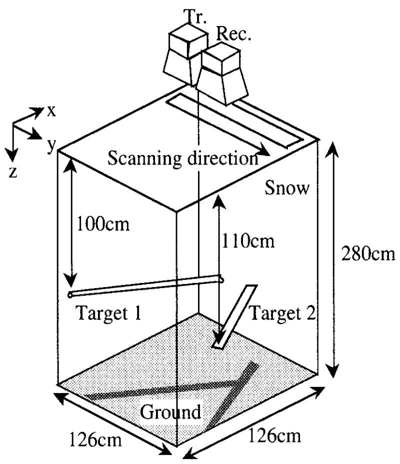

Fig. 7 Measurement situation 2.

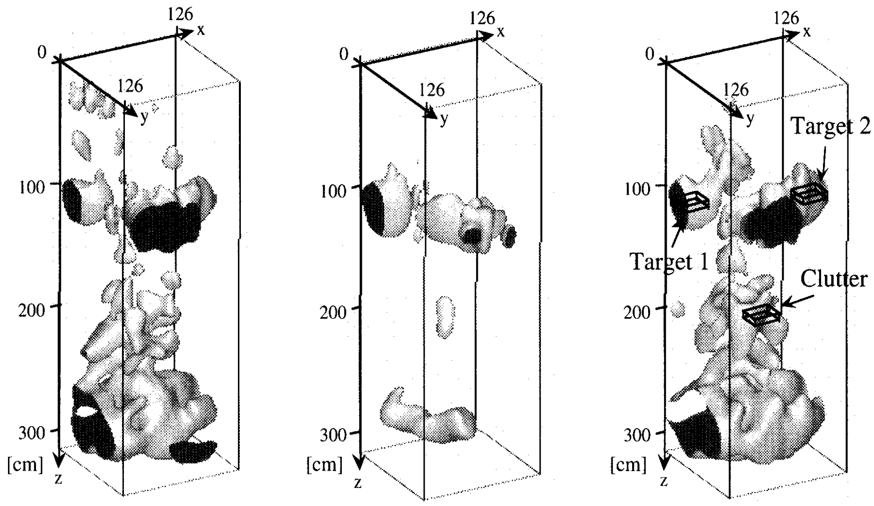

(a) HH (b) HV (c) VV

Fig. 8 Three-dimensional image of experiment 2.

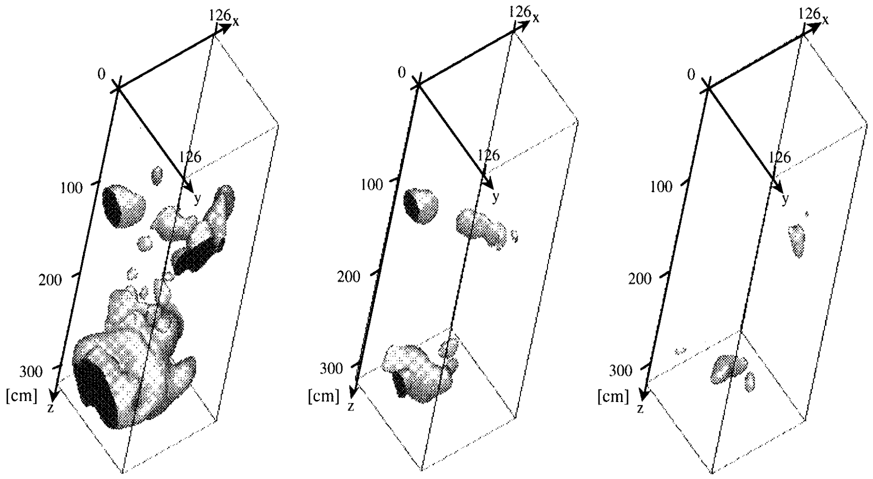

(a) Sphere (b) Diplane (c) Helix

Fig. 9 The result of three-component decomposition technique.

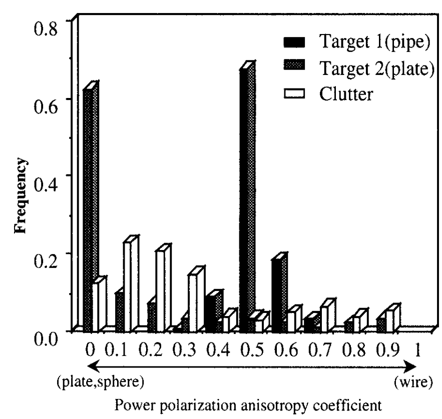

Fig. 10 The distribution of power polarization anisotropy coefficient.

cally the sphere component and diplane component with the ratio of 1:1 similar to the wire. This characteristic applies to target 1. On the other hand, the plate bar, target 2, in this measurement was decomposed into a sphere component, because the *HV* component of target is small compared to the *VV* and *HH* components. This experimental result indicates that target 2 is close to plate. Therefore, it is useful to interpret the difference of polarimetric scattering property between targets.

The power polarization anisotropy approach to classify target is applied to this measurement situation. Figure 10 shows histogram of power polarization anisotropy coefficient in the neighborhood of each target(target 1:14×8×1 pixels, target 2:8×10×1 pixels) and clutter(12×14×1 pixels). It is seen that clutter appears under the depth of 170 cm in Fig. 8. This clutter seems to be caused by snow removal by shovelling machine aprior to the measurement. The anisotropy coefficient result of targets supports three-component decomposition result. The polarization anisotropy coefficient of clutter is more uniformly distributed than that of targets in Fig. 10. Therefore, this coefficient can be used to discriminate the man-made polarization sensitive target and clutter.

5. Conclusion

This paper discussed three-dimensional polarimetric SAR image in snowpack obtained by an FM-CW radar operating in the L-band. It is first trial to obtain three-dimensional polarimetric data in inhomogeneous medium and to apply the polarimetric processing to this three-dimensional polarimetric data of buried objects. The experiment was carried out to detect buried targets at Yamakoshi village, Niigata prefecture, Japan. We tried the three-dimensional polarimetric detection at two situations. Since this radar could clearly map the buried targets, the ground surface and also the inhomogeneity of snowpack, it is useful to know the buried situation and target type. Moreover, we applied the polarimetric processings based on a three-component decomposition technique, power polarization anisotropy coefficient and polarimetric filtering to experimental results. The polarimetric filtering was useful to enhance and eliminate the target. The three-component decomposition technique provided the difference of polarimetric property of plate bar and cylinder targets. The power polarization anisotropy coefficient showed the capability to discriminate target and clutter. Therefore, these results support the usefulness of three-dimensional polarimetric FM-CW SAR.

Acknowledgment

This work was supported in part by a Grant-in-Aid for Scientific Research of the Ministry of Education, Japan.

References

[1] Y. Yamaguchi, M. Mitsumoto, M. Sengoku, and T. Abe, "Synthetic aperture FM-CW radar applied to the detection of objects buried in snowpack," IEEE Trans. Geosci. & Remote Sensing, vol.32, no.1, pp.11-18, Jan. 1994.

[2] Y. Yamaguchi, T. Nishikawa, and W.-M. Boerner, "Two-dimensional and full polarimetric imaging by a synthetic aperture FM-CW radar," IEEE Trans. Geosci. & Remote Sensing, vol.33, no.2, pp.421-427, March 1995.

[3] M. Nakamura, Y. Yamaguchi, and H. Yamada, "Real-time and full polarimetric FM-CW radar and its application to the classification of targets," IEEE Trans. Instrum. & Meas., vol.47, no.2, pp.572-577, April 1998.

[4] Y. Yamaguchi and T. Moriyama, "Polarimetric detection of objects buried in snowpack by a synthetic aperture FM-CW radar," IEEE Trans. Geosci. & Remote Sensing, vol.34, no.1, pp.45-51, Jan. 1996.

[5] W.-M. Boerner, W.L. Yan, A.Q. Xi, and Y. Yamaguchi, "On the basic principles of radar polarimetry: Huynen's polarization fork concept and its extension to the partially polarized case," Proc. IEEE, vol.79, no.10, pp.1538-1550, Oct. 1991.

[6] A.I. Kozlov and A.I. Logvin, "Theoretical and experimental results of applying the methods of radiopolarimetry in active radiolocation," Proc. ISNCR-94, pp.325-333, Nov. 1994.

[7] E. Krogager, W.-M Boerner, and S.N. Madsen, "Feature-motivated Sinclair matrix (sphere/ diplane/ helix) decomposition and its application to target sorting for land feature classification," Proc. SPIE, vol.3120, pp.144-154, Aug. 1997.

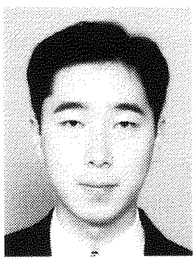

Toshifumi Moriyama was born in Fukui Prefecture, Japan, on January 1, 1972. He received the B. E., M. E. and Ph.D. degrees in Information Engineering from Niigata University, Japan, in 1994, 1995 and 1998, respectively. He is now with Fujitsu System Integration Laboratories Ltd. He was engaged in radar polarimetry and polarimetric radar sensing of buried objects. Dr. Moriyama is a member of IEEE.

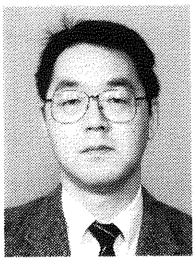

Yoshio Yamaguchi was born in Niigata, Japan, on March 12, 1954. He received the B. E. degree in electronics engineering from Niigata University in 1976, and the M. E. and Dr. Eng. degrees from Tokyo Institute Technology, Tokyo, Japan, in 1978 and 1983, respectively. In 1978, he joined the Faculty of Engineering, Niigata University, where he is a Professor. From 1988 to 1989, he was a Research Associate at the University of Illinois at Chicago. His interests are in the field of propagation characteristics of electromagnetic waves in lossy medium, radar polarimetry, microwave remote sensing and imaging. Dr. Yamaguchi is a senior member of IEEE, and a member of the Japan Society for Snow Engineering.

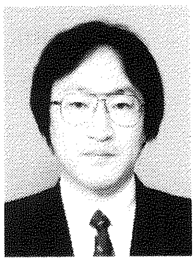

Hiroyoshi Yamada was born in Hokkaido, Japan, on November 2, 1965. He received the B.S., M. S., and Ph.D. degrees from Hokkaido University, Sapporo, Japan, in 1988, 1990, and 1993, respectively, all in electronic engineering. Since 1993, he has been with Niigata University, where he is an Associate Professor. His current research involves superresolution techniques, time-frequency analysis, electromagnetic wave measurements, and radar signal processing. Dr. Yamada is a member of IEEE.